Comparison of optical spectra of Nd^{3+} in $NdAl_3(BO_3)_4$ (NAB), $Nd:GdAl_3(BO_3)_4$ (NGAB) and $Nd:Gd_{0.2}Y_{0.8}Al_3(BO_3)_4$ (NGYAB) crystals

2001 J. Phys.: Condens. Matter 13 1171

(http://iopscience.iop.org/0953-8984/13/5/330)

INSTITUTE OF PHYSICS PUBLISHING JOURNAL OF PHYSICS: CONDENSED MATTER

J. Phys.: Condens. Matter **13** (2001) 1171–1178 www.iop.org/Journals/cm PII: S0953-8984(01)18576-0

Comparison of optical spectra of Nd^{3+} in $NdAl_3(BO_3)_4$ (NAB), Nd:$GdAl_3(BO_3)_4$ (NGAB) and Nd:$Gd_{0.2}Y_{0.8}Al_3(BO_3)_4$ (NGYAB) crystals

Xueyuan Chen[1,3], Zundu Luo[1], D Jaque[2], J J Romero[2], J Garcia Sole[2], Yidong Huang[1], Aidong Jiang[1] and Chaoyang Tu[1]

[1] Fujian Institute of Research on the Structure of Matter, Chinese Academy of Sciences, Fuzhou, Fujian 350002, China
[2] Departmento de Fisica de Materiales, Universidad Autonoma de Madrid, Cantoblanco, 28049 Madrid, Spain

E-mail: xchen@ms.fjirsm.ac.cn (Xueyuan Chen)

Received 1 November 2000

Abstract

A comparative study of the optical absorption and luminescence of crystals of $NdAl_3(BO_3)_4$ (NAB), Nd:$GdAl_3(BO_3)_4$ (NGAB) and Nd:$Gd_{0.2}Y_{0.8}Al_3(BO_3)_4$ (NGYAB) is presented. The Judd–Ofelt theory is applied to the fitting of experimental absorption line strengths to obtain the intensity parameters Ω_t ($t = 2, 4, 6$) with root mean square errors of 11.8%, 3.8% and 8.6% for NAB, NGAB and NGYAB respectively. The intensity parameters are used to calculate the radiative transition rates, branching ratios and radiative lifetimes of Nd^{3+} ions undergoing transitions from $^4F_{3/2}$ to ^4I_J manifolds. The relevant spectroscopic parameters for laser applications (quantum efficiency and emission cross section) are also estimated. The results are compared among the three samples and other borate crystals. It is concluded that NAB is a laser crystal with high gain and thus a promising candidate for microchip laser application, while NGAB (or NGYAB) can be used as an alternative to the celebrated nonlinear laser crystal NYAB.

1. Introduction

Recently there has been a revival of interest in the growth of neodymium-doped inorganic borate crystals, because of their good laser performance and excellent nonlinear optical properties; such crystals include Nd:$Ca_4GdO(BO_3)_3$ (Nd:GdCOB) [1–4], Nd:$Ca_4YO(BO_3)_3$ (Nd:YCOB) [5–8], Nd:$LaSc_3(BO_3)_4$ (NLSB) [9–11], Nd:$YAl_3(BO_3)_4$ (NYAB) [12–14], Nd:$GdAl_3(BO_3)_4$ (NGAB) [15], Nd:$Gd_xY_{1-x}Al_3(BO_3)_4$ (NGYAB) [16], $NdAl_3(BO_3)_4$ (NAB) [17–20] and $NdSc_3(BO_3)_4$ (NSB) [21]. These crystals can be developed as ideal self-frequency-doubling (SFD), self-sum-frequency-mixing (SSFM) or microchip laser materials for a wide variety of

[3] Author to whom any correspondence should be addressed. Fax: 86-591-3714946.

0953-8984/01/051171+08$30.00

applications—for example, in integrated optical communication systems, compact red–green–blue (RGB) diode-pumped solid-state lasers and laser displays.

The self-activated crystal, NAB, is a high-Nd-concentration stoichiometric laser crystal with low threshold, high gain and good physical and chemical properties. Therefore NAB is a promising candidate for diode-pumped microchip laser application [17]. It is well known that the application of NYAB crystal has been limited since it is difficult to grow large crystals with good optical quality. Thus, much attention has been focused on searching for new members of the NYAB family with comparable laser and nonlinear optical properties. NGAB and NGYAB crystals have emerged as good alternatives to NYAB. Because the radius of the Gd^{3+} ion (0.102 nm) is closer to that of the Nd^{3+} ion (0.103 nm) than that of the Y^{3+} ion (0.093 nm), it is easier to dope the Nd^{3+} into the NGYAB (or NGAB) lattice than into the NYAB lattice, which indicates that it is easier to grow homogeneous crystals of NGAB or NGYAB than NYAB [15, 16]. As reported previously, NGAB and NGYAB crystals with good optical quality have been grown by the flux method [15, 16]. In spite of the fact that the crystal growth and laser performance of NAB, NGAB and NGYAB have been demonstrated, detailed calculation of the spectroscopic parameters, such as intensity parameters, radiative transition rates and branching ratios, is still lacking. Obtaining these parameters is necessary in order to attain a full understanding of the laser gain properties, as well as to predict performance.

In this paper, we describe measurement of the absorption and fluorescence spectra of the samples and apply the Judd–Ofelt (JO) theory [22], a standard tool for quantitatively calculating the rates of parity-forbidden electric dipole (ED) transition between various manifolds of rare earths in both crystalline and glass hosts, to investigate the spectroscopic characteristics of Nd^{3+} in NAB, NGAB and NGYAB crystals.

2. Experimental procedure

Single crystals of NAB, NGAB and Nd:$Gd_{0.2}Y_{0.8}Al_3(BO_3)_4$ (NGYAB; in this paper $x = 0.2$) were grown by the flux method using a modified molybdate flux system. Details of the flux composition and growth procedure have been described in previous work [15, 16, 18, 19]. The space groups for the NAB, NGAB and NGYAB crystals are $C2/c$, $R32$ and $R32$, respectively. Their crystal structures are similar to each other and belong to the huntite structure group [23]. The site symmetries of the Nd ions are the C_2, D_3 and D_3 point groups for NAB, NGAB and NGYAB, respectively. The Nd concentrations incorporated into the crystals were 5.43×10^{21} cm^{-3} (100 at.%) for NAB, 1.59×10^{20} cm^{-3} (2.96 at.%) for NGAB and 2.21×10^{20} cm^{-3} (4 at.%) for NGYAB, respectively. The samples of NAB, NGAB and NGYAB were cut from the as-grown crystals and polished, with thicknesses of 0.15 mm, 5.5 mm and 1.3 mm, respectively.

The spectroscopic experiments were carried out at the Department of Materials Physics, Universidad Autonoma de Madrid. The unpolarized absorption spectrum of the NGYAB sample was measured with a Hitachi Spectrophotometer (model U-3501), while the polarized absorption spectra of the NAB sample were recorded by adding a calcite polarizer. The fluorescence spectra were acquired by exciting the sample with a CW Ti:sapphire laser (Spectra Physics 3900) pumped by an Ar^+ laser. Emission from the crystal was dispersed by a 500M SPEX monochromator (spectral resolution ~ 0.05 nm) and detected with a cooled photomultiplier or Ge detector. The signals were recorded by using a SR400 two-channel gated photon counter. The unpolarized absorption spectrum of the NGAB sample was recorded by a Cary 2390 spectrophotometer at Fujian Institute of Research on the Structure of Matter. All of the measurements were carried out at room temperature (RT).

3. Results and discussion

The RT absorption spectra for the NAB, NGAB and NGYAB crystals over the range of 300–950 nm are shown and compared in figure 1. The measured absorption line strengths S_{mea} for transitions from the ground $^4I_{9/2}$ manifold ($J = 9/2$) to the excited J'-manifold can be obtained from the RT absorption spectra using the following expression:

$$S_{mea}(J \rightarrow J') = \frac{3ch(2J+1)}{8\pi^3 n_{Nd}\bar{\lambda}e^2}\frac{9n}{(n^2+2)^2}\Gamma \tag{1}$$

where n_{Nd} is the Nd^{3+} concentration, n is the refractive index of the sample, $\bar{\lambda}$ is the mean wavelength of the absorption band and Γ is the integrated absorbance for each absorption band, which can be expressed as

$$\Gamma = \frac{\ln 10}{L}\int_{J\rightarrow J'} \mathrm{OD}(\lambda)\,\mathrm{d}\lambda \tag{2}$$

where $\mathrm{OD}(\lambda)$ is the measured optical density as a function of wavelength and L is the crystal thickness. When two or more absorption bands were found to be overlapped, the total integrated absorbance of the bands was treated as a single experiment point. For NAB, to take into account the anisotropic effects, an average integrated absorbance $\bar{\Gamma}$ over the σ- and π-polarized spectra was adopted; it is given by the formula $\bar{\Gamma} = (2\Gamma_\sigma + \Gamma_\pi)/3$ [24]. The refractive indices n are 1.75, 1.76 and 1.76 for NAB, NGAB and NGYAB respectively. According to JO theory, the absorption line strength for the ED transition can also be expressed in terms of the parameters $\Omega_{2,4,6}$ as

$$S_{cal}(J \rightarrow J') = \sum_{t=2,4,6} \Omega_t |\langle \Phi J||U^{(t)}||\Phi' J'\rangle|^2. \tag{3}$$

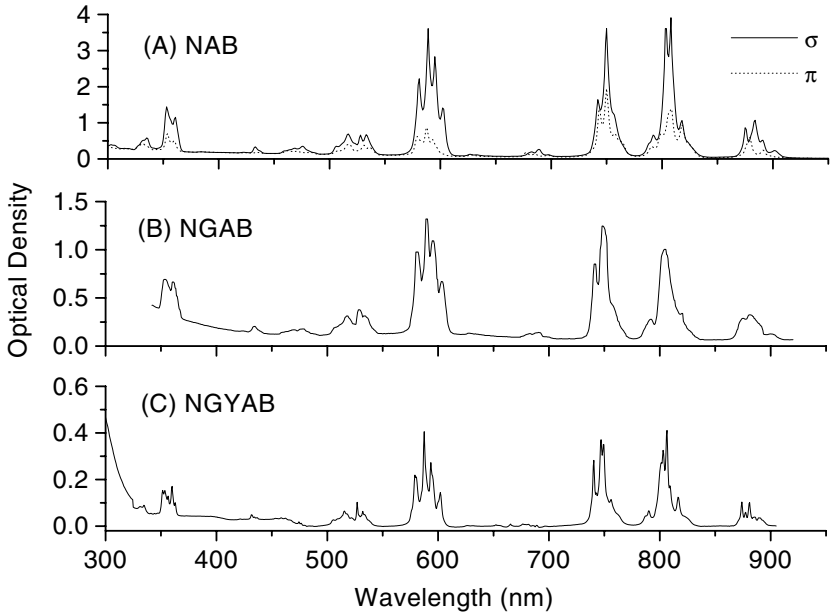

Figure 1. The RT absorption spectra of NAB, NGAB and NGYAB crystals with crystal thicknesses of 0.15 mm, 5.5 mm and 1.3 mm, respectively. The polarized (σ and π) spectra are for NAB, while the unpolarized spectra are for NGAB and NGYAB.

The reduced tensor matrix elements $|\langle \Phi J||U^{(t)}||\Phi' J'\rangle|^2$ can be found from reference [25]. By a least-squares fitting of S_{cal} to the measured line strengths S_{mea}, the parameters $\Omega_{2,4,6}$ were obtained. The values of the measured and calculated line strengths for NAB, NGAB and NGYAB are listed in table 1. The parameters $\Omega_{2,4,6}$ obtained from the fitting for the three crystals are compared in table 2. The root mean square (rms) deviation between the experimental and calculated line strengths is defined by

$$\text{rms } \Delta S = \sqrt{\sum_{i=1}^{N} (S_{mea} - S_{cal})^2 \Big/ (N-3)} \tag{4}$$

where N is the number of absorption bands. A measurement of the relative error is given by

$$\text{rms error} = \text{rms } \Delta S / \text{rms } S \times 100\% \tag{5}$$

where

$$\text{rms } S = \sqrt{\sum_{i=1}^{N} S_{mea}^2 \Big/ N}.$$

The values of rms ΔS and 'rms error' for the three crystals are also presented in table 1. The values of 'rms error' for the fitting are 11.8%, 3.8% and 8.6% for the NAB, NGAB and NGYAB crystals respectively, which indicates that the fitting results are in good agreement with the experiments.

Table 1. The measured and calculated $^4I_{9/2}$ absorption line strengths for NAB, NGAB and NGYAB crystals. (Note: all values of S_{mea} and S_{cal} are in units of 10^{-20} cm^2. A dash indicates that the absorption band is not included in the fit.)

		NAB		NGAB		NGYAB	
J-manifold	$\bar{\lambda}$ (nm)	S_{mea}	S_{cal}	S_{mea}	S_{cal}	S_{mea}	S_{cal}
$^4F_{3/2}$	884	3.27	2.90	0.99	1.06	0.85	0.90
$^4F_{5/2} + {}^2H2_{9/2}$	808	10.53	9.77	3.22	3.27	3.46	3.36
$^4F_{7/2} + {}^4S_{3/2}$	750	9.35	10.03	3.24	3.22	3.43	3.57
$^4F_{9/2}$	688	0.91	0.70	—	—	0.19	0.24
$^2H2_{11/2}$	628	0.38	0.18	—	—	—	—
$^4G_{5/2} + {}^2G1_{7/2}$	588	12.30	12.32	5.64	5.65	4.56	4.58
$^2K_{13/2} + {}^4G_{7/2} + {}^4G_{9/2}$	520	4.45	4.25	1.69	1.58	1.85	1.43
$^2K_{15/2} + {}^2G1_{9/2} + {}^2D1_{3/2} + {}^4G_{7/2}$	470	1.53	0.94	0.47	0.33	—	—
$^2P_{1/2} + {}^2P1_{5/2}$	434	0.62	0.37	—	—	0.15	0.11
$^4D_{3/2} + {}^4D_{5/2} + {}^4D_{1/2} + {}^2I_{11/2} + {}^2I_{15/2}$	355	5.31	5.90	—	—	1.64	1.79
$^2I_{13/2} + {}^4D_{7/2} + {}^2L_{17/2}$	334	1.68	0.21	—	—	0.22	0.07
rms ΔS (10^{-20} cm^2)		0.726		0.118		0.206	
rms error (%)		11.8		3.8		8.6	

Once the parameters $\Omega_{2,4,6}$ have been determined, the ED radiative transition rate $A(J \to J')$, corresponding to transitions from $^4F_{3/2}$ to the lower manifolds $^4I_{9/2,11/2,13/2,15/2}$, can be calculated using the following equation:

$$A(J \to J') = \frac{64\pi^4 e^2}{3h(2J+1)\bar{\lambda}^3} \frac{n(n^2+2)^2}{9} \sum_{t=2,4,6} \Omega_t |\langle {}^4F_{3/2}||U^{(t)}||{}^4I_{J'}\rangle|^2 \tag{6}$$

Table 2. Comparison of the spectroscopic parameters of NAB, NGAB, NGYAB and other Nd^{3+}-doped borate crystals. ($\Omega_{2,4,6}$, $\sigma_{1.06}$ and $\sigma_{1.34}$ are in units of 10^{-20} cm^2. A dash indicates that the data are not currently available.)

Crystal	Ω_2	Ω_4	Ω_6	τ_f (μs)	τ_r (μs)	η (%)	$\sigma_{1.06}$	$\sigma_{1.34}$	Reference
NAB	6.07	9.14	14.58	16[a]	98	16.3	28.4	9.3	This work
NGAB	3.35	3.50	4.64	50[b]	285	17.5	17.6	—	This work
NGYAB	2.71	2.68	5.22	(54)[c]	294	18.4	(18.5)[d]	—	This work
NYAB	3.09	5.04	3.11	56	302	18.5	18.0	3.0	Reference [12]
Nd:GdCOB	1.07	2.64	1.52	98	659	15.0	4.2	—	Reference [4]
α-NLSB	3.92	4.41	4.14	112	225	49.8	13.0	5.1	Reference [9]
β-NLSB	2.85	3.69	4.73	112	226	49.4	16.0	—	Reference [10]

[a] Reference [17].
[b] Reference [20].
[c] Value interpolated between NYAB and NGAB, to be determined by a future fluorescence experiment.
[d] Predicted value determined from the ratio of the corresponding transition rates of NGAB and NGYAB, assuming that they have the same emission linewidth at 1.06 μm.

where $|\langle {}^4F_{3/2}||U^{(t)}||{}^4I_{J'}\rangle|^2$ were given in reference [26]. Then, the radiative lifetime and branching ratios for ${}^4F_{3/2}$, which are relevant to the laser performance, can be estimated from the following relations:

$$\tau_r = 1\Big/\sum_{J'} A(J \to J')$$

$$\beta_{J\to J'} = A(J \to J')\Big/\sum_{J'} A(J \to J').$$

The radiative quantum efficiency is defined as $\eta = \tau_f/\tau_r$, where τ_f is the fluorescence lifetime. The calculated radiative transition rates and branching ratios for the three crystals are shown in table 3. The values reported for the NYAB crystal are also included in that table for comparison. The spectral dependence of the stimulated emission (SE) cross section for the laser channel from ${}^4F_{3/2}$ to ${}^4I_{11/2}$ can be determined from its RT fluorescence spectrum according to [12]

$$\sigma_\lambda = \lambda^5 \beta_{J\to J'} I(\lambda)\Big/\left(8\pi n^2 c\tau_r \int \lambda I(\lambda)\,\mathrm{d}\lambda\right) \tag{7}$$

where λ is the emission wavelength, $I(\lambda)$ the fluorescent intensity as a function of wavelength, c the speed of light and n the crystal refractive index. The SE cross sections as functions of laser wavelength for the NAB and NGAB crystals are shown and compared in figure 2. Due to the lack of a fluorescence spectrum for the NGYAB crystal, the calculation of its emission

Table 3. Comparison of the radiative transition rates and branching ratios for the ${}^4F_{3/2} \to {}^4I_J$ transitions of NAB, NGAB, NGYAB and NYAB crystals.

		NAB		NGAB		NGYAB		NYAB[a]	
Transition	$\bar{\lambda}$ (μm)	A (s^{-1})	β (%)	A (s^{-1})	β (%)	A (s^{-1})	β (%)	A (s^{-1})	β (%)
${}^4F_{3/2} \to {}^4I_{9/2}$	0.88	3737	36.7	1380	39.4	1141	33.5	1637	49.3
${}^4F_{3/2} \to {}^4I_{11/2}$	1.06	5284	51.8	1759	50.2	1841	54.1	1430	43.1
${}^4F_{3/2} \to {}^4I_{13/2}$	1.34	1121	11.0	349	10.0	404	11.9	235	7.1
${}^4F_{3/2} \to {}^4I_{15/2}$	1.87	53	0.5	17	0.4	19	0.5	12	0.5

[a] Reference [12].

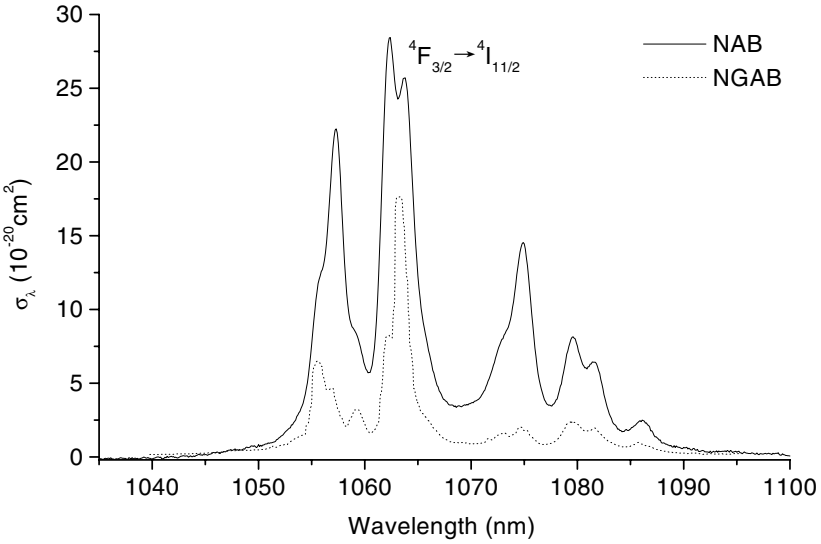

Figure 2. The spectral dependence of the stimulated emission cross section calculated from the RT $^4F_{3/2} \rightarrow {}^4I_{11/2}$ fluorescence spectrum for the NAB and NGAB crystals.

cross section has not been carried out yet (however, an approximate value is predicted in table 2 for comparison). All of the spectroscopic parameters ($\Omega_{2,4,6}$, τ_r, τ_f, η, σ_λ) for NAB, NGAB and NGYAB are listed and compared with those for other borate crystals in table 2.

Having compared the spectroscopic parameters with each other, we found that the NAB crystal has the largest intensity parameters $\Omega_{2,4,6}$ (table 2) and thus radiative transition rates for $^4F_{3/2} \rightarrow {}^4I_J$ (table 3). According to the JO theory, the intensity parameters depend strongly on the values of the odd-parity crystal-field parameters originating from the non-centrosymmetry interaction of the crystal field. Thus we may compare the local structures of Nd ions among NAB, NGAB, NGYAB and NYAB. As stated in section 2, in fact the Nd ions in NAB occupy C_2 symmetry positions rather than D_3 ones because of a small structural distortion from the D_3 group. Hence the least symmetric structure among the crystals considered here is that of NAB, in which the inverse position of any near-neighbour O atom is far removed from any other O near neighbour. This lack of site inversion symmetry enables the odd-parity crystal-field components to admix the opposite-parity $4f^2 5d$ configuration with the $4f^3$ configuration of Nd^{3+}, making the forced ED transitions within the predominantly $4f^3$ configuration much more favoured. This is also the major reason for the largest radiative transition rates being those for $^4F_{3/2} \rightarrow {}^4I_{9/2,11/2,13/2}$ and the shortest radiative lifetime being that of $^4F_{3/2}$ in NAB, as shown in tables 2 and 3. The calculated branching ratios for $^4F_{3/2} \rightarrow {}^4I_{9/2,11/2,13/2}$ in NAB are 36.7%, 51.8% and 11%, respectively, in good agreement with the experimental values (36%, 50% and 14%) determined from the calibrated fluorescence spectra [17]. The calculated peak SE cross sections for $^4F_{3/2} \rightarrow {}^4I_{11/2}$ in the NAB crystal is $\sigma_{1.06} = 2.84 \times 10^{-19}$ cm^2 (figure 2), which agrees well with the experimental value determined from the laser performance ($\sigma_{1.06} = 3.0 \times 10^{-19}$ cm^2) [17]. Furthermore, the peak SE cross sections for $^4F_{3/2} \rightarrow {}^4I_{13/2}$ in NAB are also calculated; the value obtained is $\sigma_{1.34} = 9.3 \times 10^{-20}$ cm^2. This value is higher than that determined from laser experiments ($\sim 5.0 \times 10^{-20}$ cm^2) [17] because the latter is the net gain cross section obtained by subtracting the excited-state absorption (ESA) cross section, supposing that the ESA of the 1.34 μm laser from $^4F_{3/2}$ is not negligible in NAB.

As expected, the spectroscopic parameters of NGAB and NGYAB are similar to those of NYAB; that is, their parameters $\Omega_{2,4,6}$ are in the range (3–5) $\times 10^{-20}$ cm^2, the fluorescence lifetimes are 50–56 μs, the radiative lifetimes are around 300 μs, the radiative quantum efficiencies are about the same ($\sim$18%) and the emission cross sections for 1.06 μm are close to 2×10^{-19} cm^2. These similarities can be explained well if one recalls that the structures of NGAB, NGYAB and NYAB crystals have the same space group and Nd site symmetry except for a slight variation of the unit-cell parameters.

In table 2, it is remarkable that the radiative quantum efficiency is very low for Nd-doped borate crystals (all below 18.5%, except for NLSB with a value of about 50%). It is well known that the highest phonon frequency associated with the main oscillation bands of the planar group $(BO_3)^{3-}$ is generally as high as about 1300–1400 cm^{-1}. The highest-energy phonons are usually considered to make the dominant contribution to the multiphonon relaxation from the $^4F_{3/2}$ state to the next lower state $^4I_{15/2}$ since they can interact with electrons to conserve energy in the lowest-order process. Thus the multiphonon nonradiative relaxation rate is generally larger in the borate family than in others, which leads to the low quantum efficiency. The reason for the difference in radiative quantum efficiency between the NYAB (about 18%) and NLSB (about 50 %) families may be that the NdO_6 complexes are isolated from each other by a longer Nd–Nd distance in the NLSB lattices than in NAB families, as can be seen from the structural analysis, and thus the comparatively isolated NdO_6 complexes in NLSB crystals could result in smaller quenching effects as well as a long fluorescence lifetime (112 μs), as also indicated by Wang *et al* [9].

4. Conclusions

A spectroscopic investigation of Nd^{3+} in NAB, NGAB and NGYAB crystals has been performed. By using the JO theory to fit the experimental absorption line strengths and fluorescence spectra, we obtained the intensity parameters $\Omega_{2,4,6}$, as well as other spectroscopic parameters that relate to laser performance. The results are compared with each other for the Nd-doped borate crystals. We found that NAB has good spectroscopic and laser properties, which show that NAB is a highly efficient laser material and thus a promising candidate for microchip laser applications. Since NGAB and NGYAB are quite similar to NYAB as regards spectroscopic properties and the former are easier to grow than the latter, NGAB and NGYAB can be regarded as good substitutes for NYAB as SFD or SSFM laser crystals.

Acknowledgments

This project was supported by the NSFC (No 60088004), Fujian Provincial Natural Science Foundation of China (No A9910019), Fujian Provincial International Cooperation Foundation of China (No 99-I-7) and the Foundation of the Chinese Academy of Sciences for Outstanding Returned Scholars.

References

[1] Aka G *et al* 2000 *J. Alloys Compounds* **303–304** 401
[2] Mougel F, Aka G, Kahn-Harari A and Vivien D 1999 *Opt. Mater.* **13** 293
[3] Aka G *et al* 1998 *J. Opt. Soc. Am.* B **14** 2238
[4] Mougel F *et al* 1997 *Opt. Mater.* **8** 161
[5] Chen C T *et al* 2000 *J. Opt. Soc. Am.* B **17** 566
[6] Eichenholz J M *et al* 1999 *Appl. Phys. Lett.* **74** 1954

[7] Ye Q and Chai B H T 1999 *J. Cryst. Growth* **197** 228
[8] Iwai M, Kobayashi T, Furuya H, Mori Y and Sasaki T 1997 *Japan. J. Appl. Phys.* II **36** L276
[9] Wang G, Chen W, Lin Z and Hu Z 1999 *Phys. Rev.* B **60** 15 469
[10] Chen W, Wang G, Lin Z and Hu Z 1999 *Opt. Commun.* **162** 49
[11] Meyn J-P, Jensen T and Huber G 1994 *IEEE J. Quantum Electron.* **30** 913
[12] Jaque D, Capmany J, Luo Z D and Garcia Sole J 1997 *J. Phys.: Condens. Matter* **9** 9715
[13] Jaque D, Capmany J, Garcia Sole J, Luo Z D and Jiang A D 1998 *J. Opt. Soc. Am.* B **15** 1656
[14] Jaque D, Capmany J and Garcia Sole J 1999 *Appl. Phys. Lett.* **75** 325
[15] Tu Chaoyang, Qiu Minwang, Huang Yichuan, Chen Xueyuan, Jiang Aidong and Luo Zundu 2000 *J. Cryst. Growth* **208** 487
[16] Tu Chaoyang, Huang Yichuan, Qiu Minwang and Luo Zundu 2000 *J. Cryst. Growth* **206** 249
[17] Jaque D, Enguita O, Garcia Sole J, Jiang A D and Luo Z D 2000 *Appl. Phys. Lett.* **76** 2176
[18] Luo Z D, Jiang A D, Huang Y and Qiu M 1991 *Sci. China* A **34** 762
[19] Wang G, He M and Luo Z D 1991 *Mater. Res. Bull.* **26** 1085
[20] Chinn S R and Hong H Y-P 1975 *Opt. Commun.* **15** 345
[21] Gruber J B, Reynolds T A, Keszler D A and Zandi B 2000 *J. Appl. Phys.* **87** 7159
[22] Judd B R 1962 *Phys. Rev.* **127** 750
Ofelt G S 1962 *J. Chem. Phys.* **37** 511
[23] Jung S T, Yoon J T and Chung S J 1996 *Mater. Res. Bull.* **31** 1021
[24] Luo Zundu, Chen Xueyuan and Zhao Tingjie 1997 *Opt. Commun.* **134** 415
[25] Carnall W T, Fields P R and Rajnak K 1968 *J. Chem. Phys.* **49** 4424
[26] Krupke W F 1974 *IEEE J. Quantum Electron.* **10** 450